Unpolarized Nucleon TMDPDFs from LQCD

Based on arXiv:2211.02340 [hep-lat]

Jinchen He

University of Maryland, College Park

June, 2023

What are TMDPDFs

- Transverse-Momentum-Dependent PDFs: the distribution densities to find a parton carrying a longitudinal momentum fraction x and transverse momentum k_T in a hadron.
- TMDPDFs can be regarded as a tomography of the hadron, which reveals the hadron's 3D internal structure.

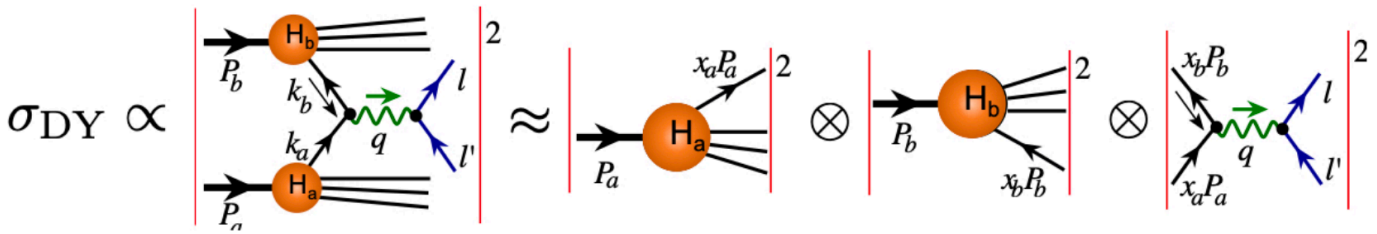

Boussarie, et al. 2304.03302

Why Care about TMDPDFs

- Understanding the inner structure of hadrons.
- TMD processes are very important processes in high energy collisions, like SIDIS on EIC.
- TMDPDFs are important inputs for experiments on TMD processes.

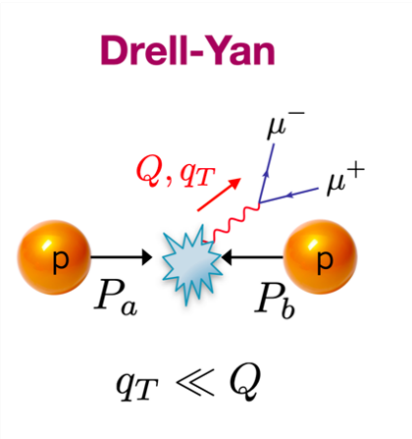

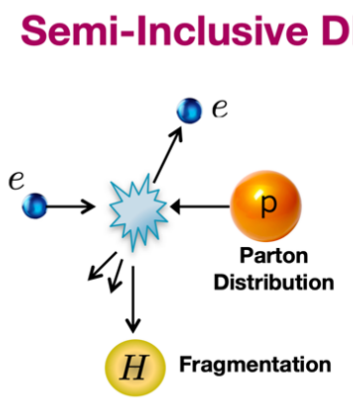

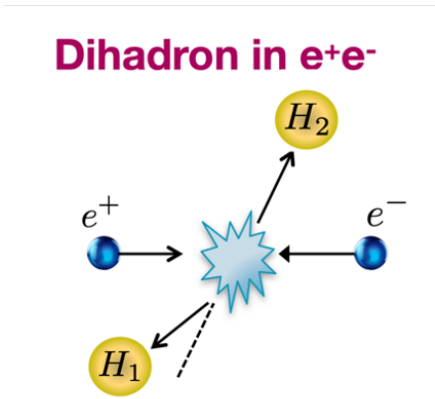

Boussarie, et al. 2304.03302

Recent Progress

- Theoretical analysis
  - TMD factorization, evolution and resummation

    Boussarie, et al. TMD handbook (2023) . . .
- Phenomenological extractions
  - Unpolarized

    Bacchetta, et al. JHEP 06 (2017); Scimem, et al. JHEP 06 (2020); Bury, et al. JHEP 10 (2022); Bacchetta, et al. JHEP 10 (2022); Moos, et al. 2305.07473 . . .
  - Sivers

    Bury, et al. PRL 126 (2021), JHEP 05 (2021); Fernando, et al. 2304.14328 . . .
  - Boer-Mulders

    Zhang, et al. PRD 77 (2008), Lu, et al. PRD 81 (2010) . . .

Recent Progress

- Lattice calculation
  - Lorentz-invariant approach: ratios of Mellin moments
    Hagler, et al. EPL 88 (2009); Musch, et al. PRD 85 (2012); Yoon, et al. 1601.05717, PRD 96 (2017) . . .
  - LaMET: formalism
    Ji, et al. PLB 811 (2020), NPB 955 (2020), RMP 93 (2021); Ebert, et al. JHEP 04 (2022); Deng, et al. JHEP 09 (2022); Ji, et al. PRD 105 (2022), 2305.04416; Ó. del Río, et al. 2304.14440 . . .
  - LaMET: soft functions
    LPC, PRL 125 (2020); Shanahan, et al. PRD 104 (2021); Schlemmer, et al. JHEP 08 (2021); Li, et al. PRL 128 (2022); LPC, PRD 106 (2022), 2306.06488 . . .
  - LaMET: renormalization and resummation
    LPC, PRL 129 (2022); Su, et al. NPB 991 (2023) . . .

LaMET

- Quasi distribution: equal time, P^z-dependent.
- Light-cone distribution: separate in time direction, universal.

$$\tilde{f}_\Gamma\left(x, b_\perp, \zeta_z, \mu\right) \sqrt{S_I\left(b_\perp, \mu\right)} = H_\Gamma\left(\frac{\zeta_z}{\mu^2}\right) e^{\frac{1}{2}\ln\left(\frac{\zeta_z}{\zeta}\right) K\left(b_\perp, \mu\right)} \times f\left(x, b_\perp, \mu, \zeta\right) + \mathcal{O}\left(\frac{\Lambda_{\mathrm{QCD}}^2}{\zeta_z}, \frac{M^2}{(P^z)^2}, \frac{1}{b_\perp^2 \zeta_z}\right)$$

Intrinsic soft function

Collins-Soper kernel

Quasi distribution

Hard kernel

Light-cone distribution

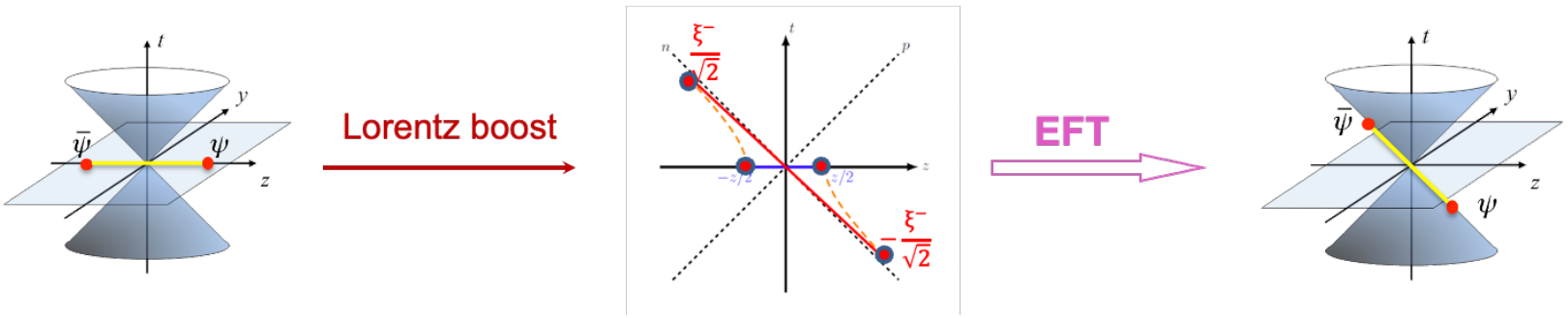

Matrix Element on the Lattice

$$\tilde{f}_\Gamma\left(x, b_\perp, P^z, \mu\right) \equiv \lim_{\substack{a\to 0 \\ L\to\infty}} \int \frac{dz}{2\pi} e^{-iz(xP^z)} \times \frac{\tilde{h}^0_\Gamma\left(z, b_\perp, P^z, a, L\right)}{\sqrt{Z_E\left(2L+z, b_\perp, a\right)} Z_O\left(1/a, \mu, \Gamma\right)}$$

$$\tilde{h}^0_\Gamma\left(z, b_\perp, P^z, a, L\right) = \langle P^z | \tilde{O}^0_{\Gamma,\sqsubset}(z, b_\perp, P^z; L) | P^z \rangle$$

$$\tilde{O}^0_{\Gamma,\sqsubset}(z, b_\perp, L) \equiv \bar{\psi}(b_\perp \hat{n}_\perp) \Gamma U_{\sqsubset,L}\left(b_\perp \hat{n}_\perp, z\hat{n}_z\right) \psi(z\hat{n}_z)$$

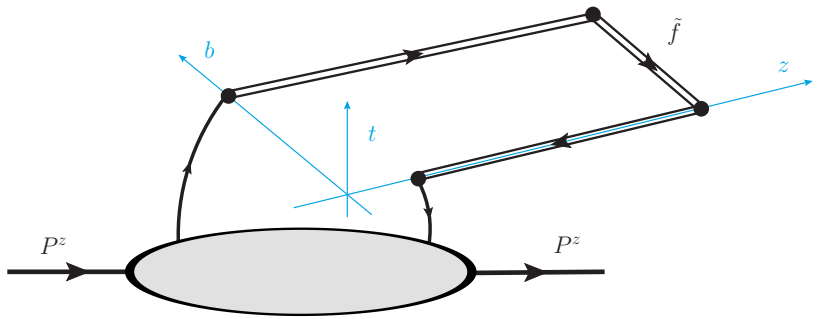

Renormalization: Divergence from Wilson links

$$\tilde{h}_\Gamma\left(z, b_\perp, P^z, a, \mu\right) = \lim_{L\to\infty} \frac{\tilde{h}^0_\Gamma\left(z, b_\perp, P^z, a, L\right)}{\sqrt{Z_E\left(2L+z, b_\perp, a\right)} Z_O(1/a, \mu, \Gamma)}$$

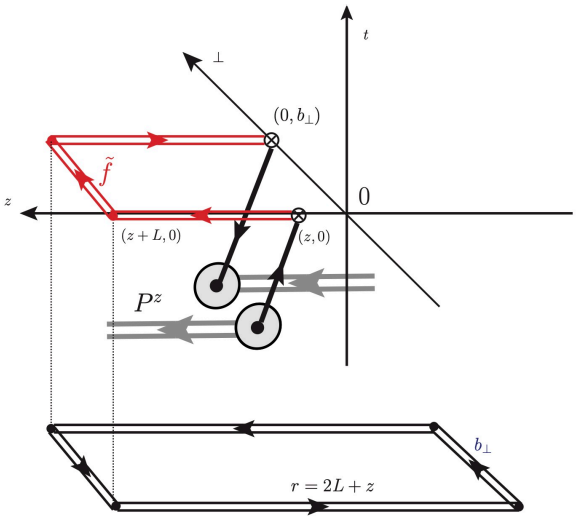

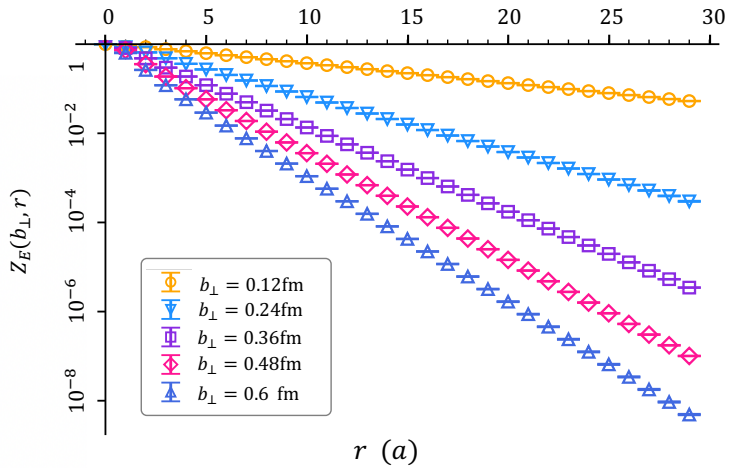

Zhang, et al. PRL 129 (2022)

Renormalization: Divergence from quark-gauge link vertices

$$\tilde{h}_\Gamma\left(z, b_\perp, P^z, a, \mu\right) = \lim_{L\to\infty} \frac{\tilde{h}^0_\Gamma\left(z, b_\perp, P^z, a, L\right)}{\sqrt{Z_E\left(2L+z, b_\perp, a\right)} Z_O(1/a, \mu, \Gamma)}$$

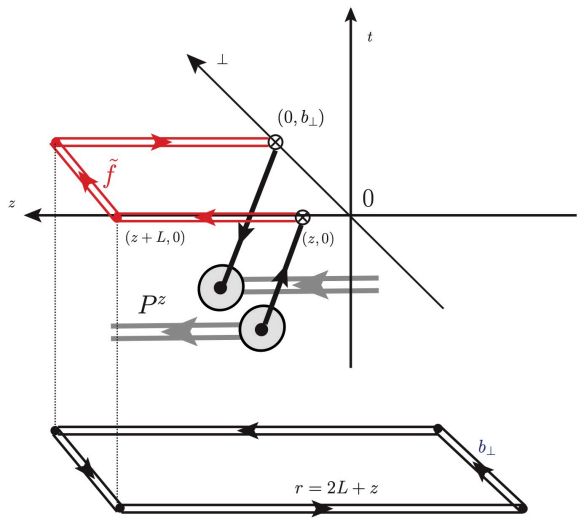

- Extract Z_O by matching the renormalized results with perturbation theory at short distance.

$$Z_O\left(1/a, \mu, \Gamma\right) = \lim_{L\to\infty} \frac{\tilde{h}^0_\Gamma\left(z, b_\perp, 0, a, L\right)}{\sqrt{Z_E\left(2L+z, b_\perp, a\right)} \tilde{h}^{\overline{\text{MS}}}_\Gamma\left(z, b_\perp, \mu\right)}$$

Zhang, et al. PRL 129 (2022)

RG Resummation: Hard kernel

The hard kernel involves some log terms, the higher orders cannot be ignored when $\zeta_z/\mu^2 = (2xP^z/\mu)^2$ is not close to 1.

$$\ln H_\Gamma^{(1)}\left(\frac{\zeta_z}{\mu^2}\right) = \frac{\alpha_s C_F}{2\pi}\left(-2 + \frac{\pi^2}{12} + \ln\frac{\zeta_z}{\mu^2} - \frac{1}{2}\ln^2\frac{\zeta_z}{\mu^2}\right)$$

$$\ln H_\Gamma^{(2)}\left(\frac{\zeta_z}{\mu^2}\right) = \alpha_s^2\left[c_2 - \frac{1}{2}\left(\gamma_C^{(2)} - \beta_0 c_1\right)\ln\frac{\zeta_z}{\mu^2} - \frac{1}{4}\left(\Gamma_{\text{cusp}}^{(2)} - \frac{\beta_0 C_F}{2\pi}\right)\ln^2\frac{\zeta_z}{\mu^2} - \frac{\beta_0 C_F}{24\pi}\ln^3\frac{\zeta_z}{\mu^2}\right]$$

Thus, evolve the fixed order result from $\mu_0 = 2xP^z$ to $\mu = 2$ GeV.

$$H\left(\zeta_z/\mu^2\right) = H\left(\zeta_z/\mu_0^2\right)\exp\left[\int_{\mu_0}^{\mu}\frac{d\mu}{\mu}\left(\Gamma_{\text{cusp}}^{(1)}\ln\frac{\zeta_z}{\mu^2}\alpha_s(\mu) + \gamma_C^{(1)}\alpha_s(\mu) + \Gamma_{\text{cusp}}^{(2)}\ln\frac{\zeta_z}{\mu^2}\alpha_s^2(\mu) + \ldots\right)\right]$$

Ji, et al. PLB 811 (2020), Su, et al. NPB 991 (2023)

RG Resummation

All perturbation results should be modified with RG resummation in the consistent way.

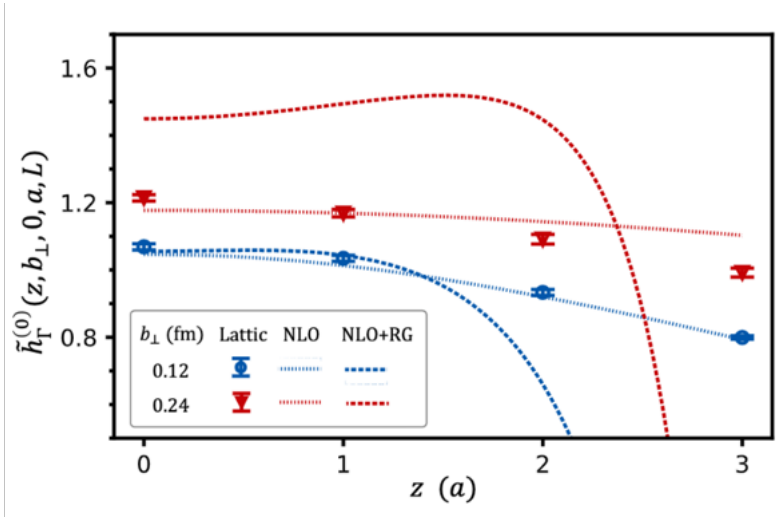

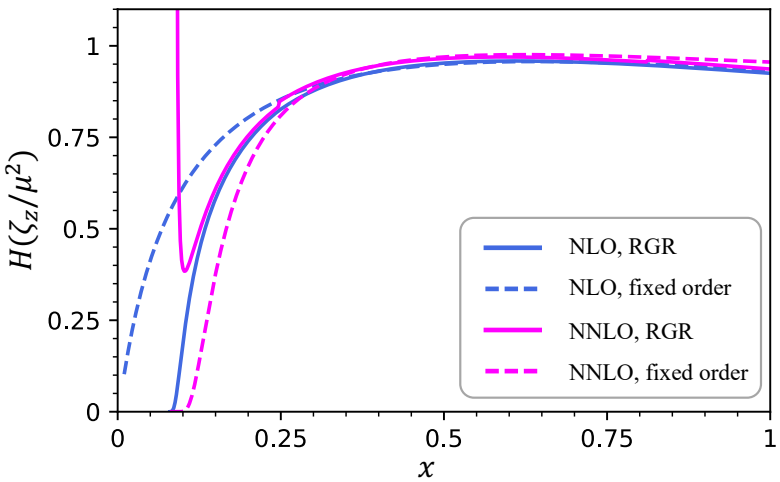

Soft Functions: CS kernel

Rapidity dependent: Collins-Soper kernel.

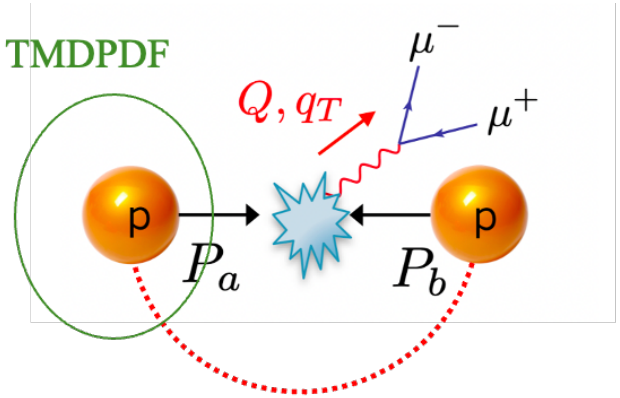

Soft gluon emission => **soft function**

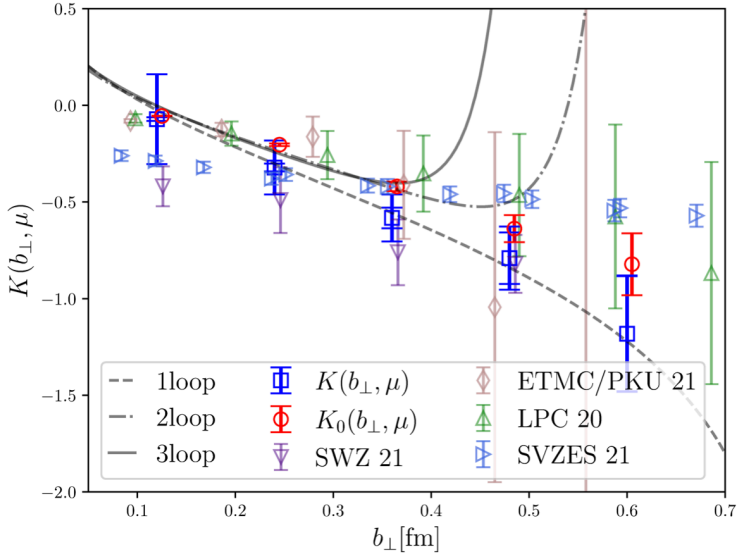

Chu(LPC), PRD 106 (2022)

Soft Functions: Intrinsic soft function

Rapidity independent: Intrinsic soft function.

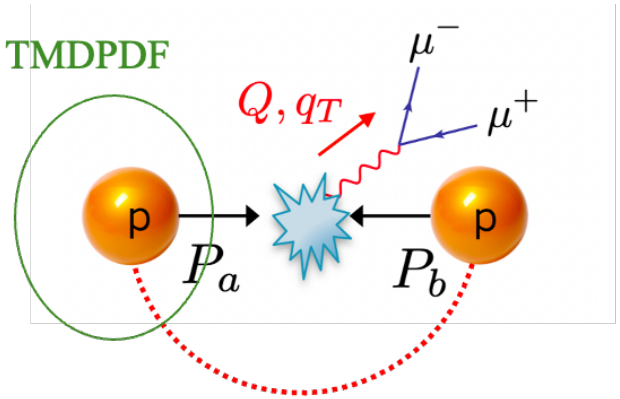

Soft gluon emission => **soft function**

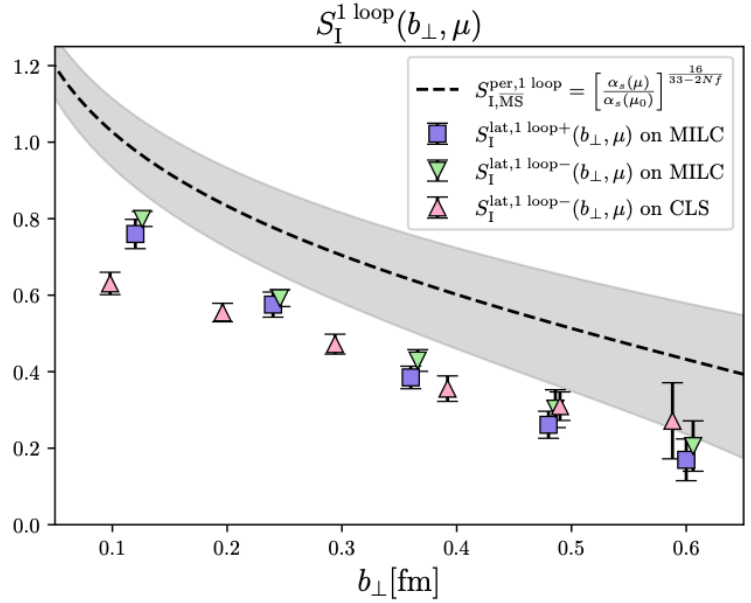

Chu(LPC), 2302.09961

Inverse Matching

Now we are prepared to get the physical TMDPDF.

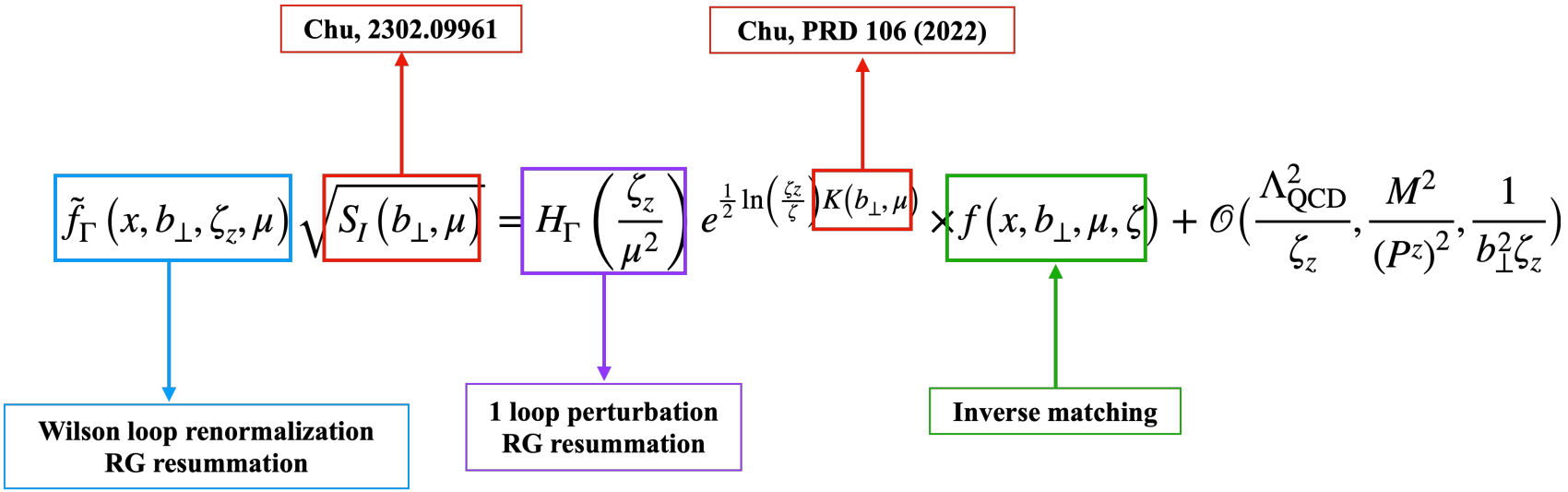

Lattice Setup

- 2+1+1 flavors of HISQ action by MILC (a=0.12 fm);
- Lattice volumn: $n_s^3 \times n_t = 48^3 \times 64$;
- Valance pion mass: 310 MeV, 220 MeV;
- Gamma structure: γ^t and γ^z;
- Hadron momentum: 1.72 GeV, 2.15 GeV, 2.58 GeV;
- Separation in the momentum direction:
  $z \in [0, 12]a = [0, 1.44]$ fm;
- Separation in the transverse direction:
  $b \in [1, 5]a = [0.12, 0.6]$ fm.

Ground State Fit: Fit quality

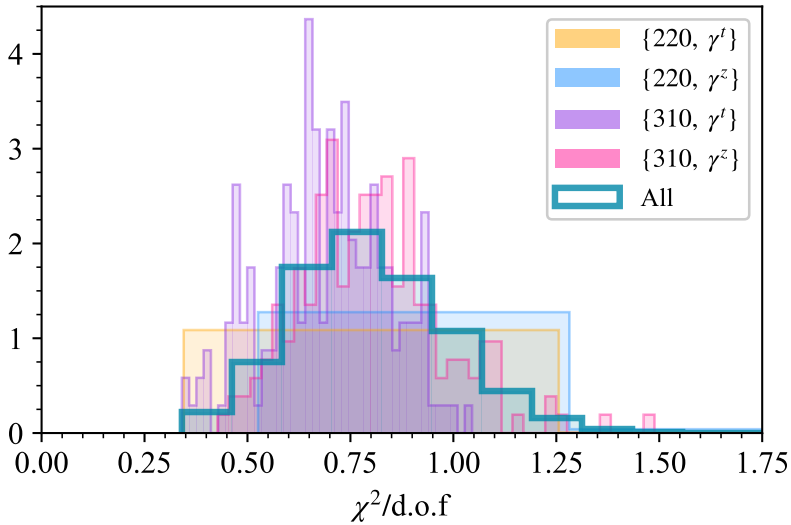

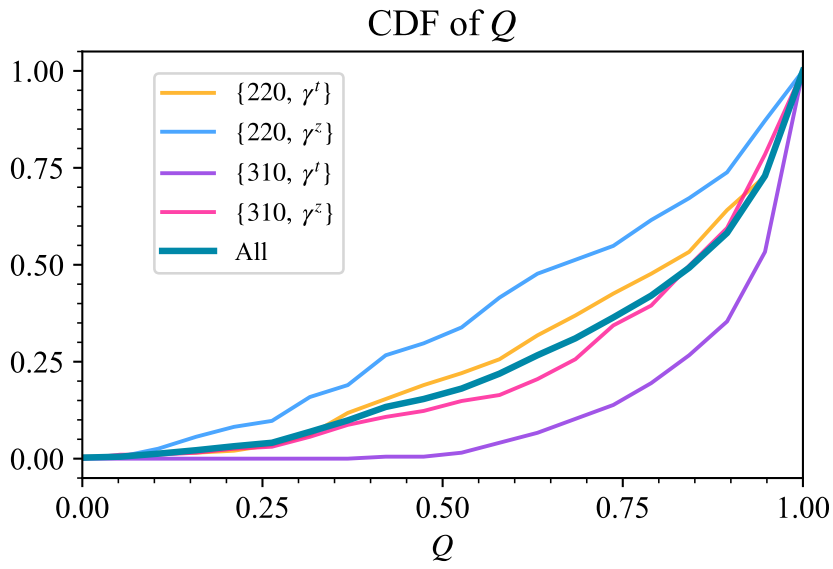

- χ^2/d.o.f. mainly distribute in the reasonable range.
- Almost no bad fits with p-value smaller than 0.05.

Renormalized Quasi Distribution in the Coordinate Space

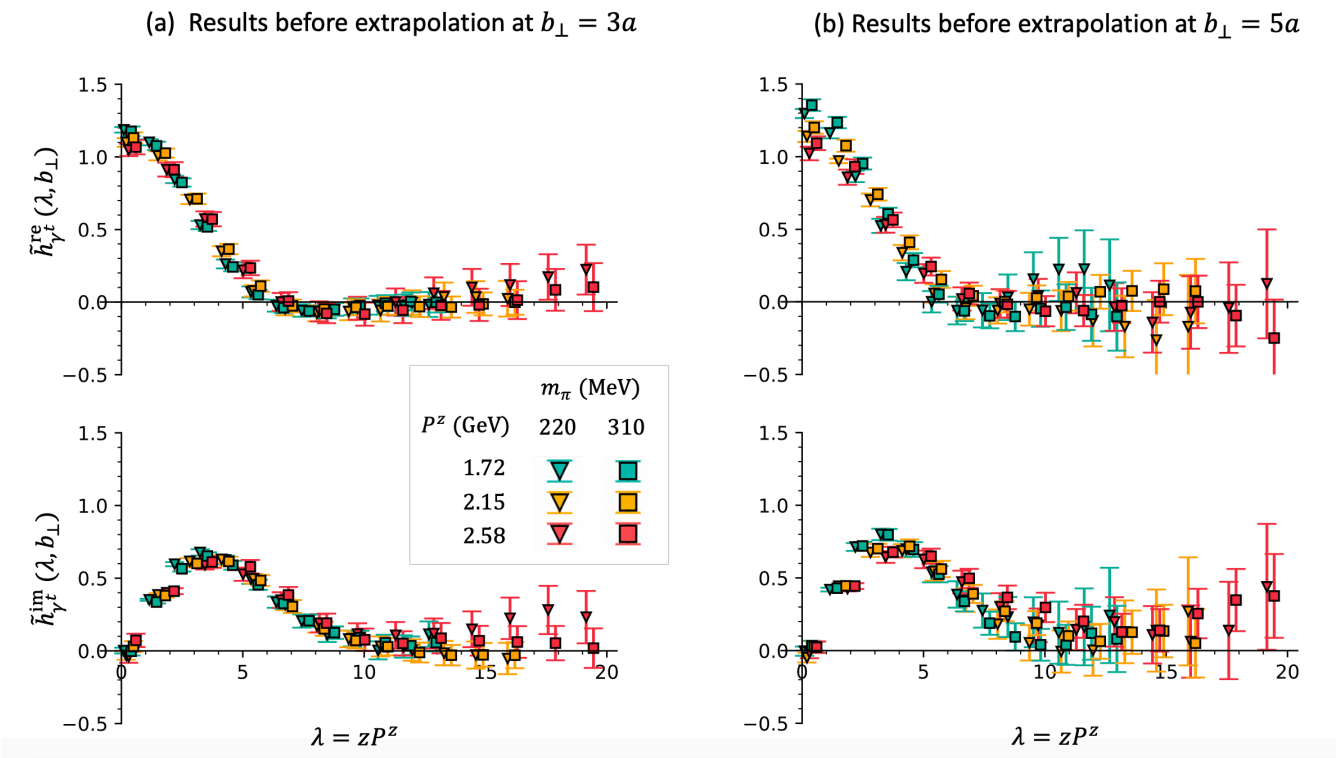

- Truncation at the finite distance.
- Tails are close to zero.

Extrapolation

The extrapolation form in the coordinate space originated from the power law behavior in the endpoint regions.

Ji, et al. NPB 964 (2021)

$$\tilde{h}_{\Gamma,\text{extra}}(\lambda) = \left[\frac{m_1}{(-i\lambda)^{n_1}} + e^{i\lambda}\frac{m_2}{(i\lambda)^{n_2}}\right] e^{-\lambda/\lambda_0}$$

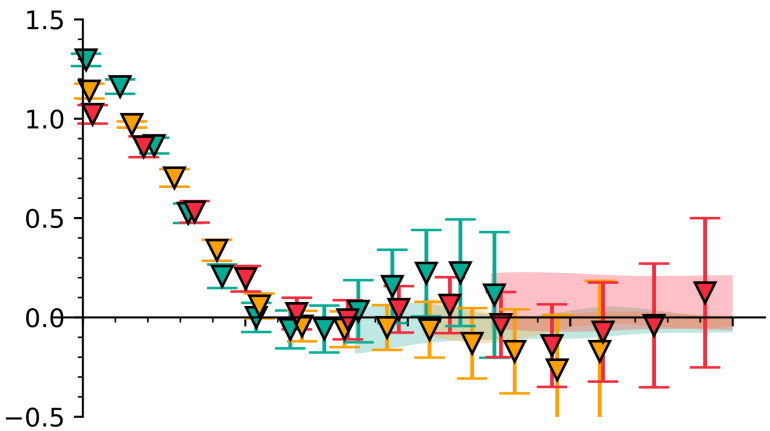

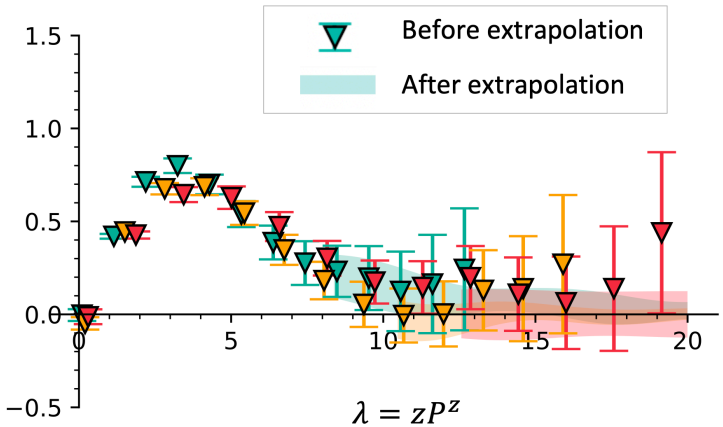

Inverse Matching

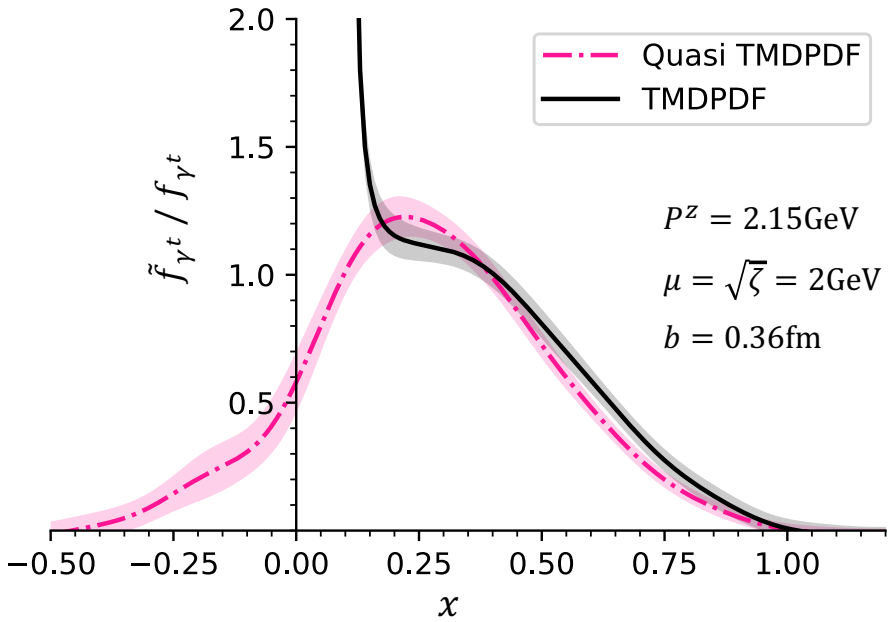

- Quasi and light-cone distributions are consistent in the reliable region.
- Near $x = 0$, the RG resummed hard kernel blows up.

Physical Limit

We did a combined extrapolation to achieve the physical limit.

$$f_\Gamma(x, b_\perp, \mu, \zeta; m_\pi, P^z) = f_\Gamma(x, b_\perp, \mu, \zeta)\Big|_{\substack{m_\pi \to m_{\pi,\text{phy}} \\ P^z \to \infty}} \times \left[1 + d_0\left(m_\pi^2 - m_{\pi,\text{phy}}^2\right) + \frac{d_1}{(P^z)^2}\right]$$

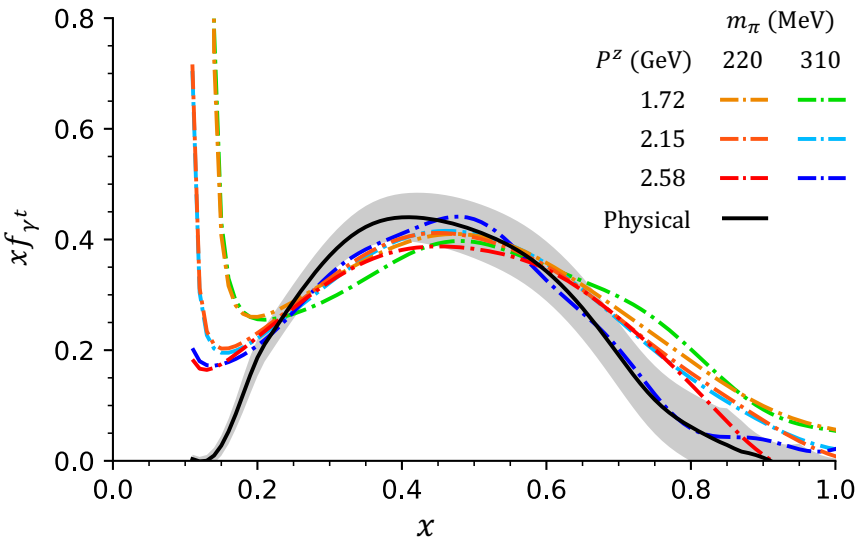

Error Estimation

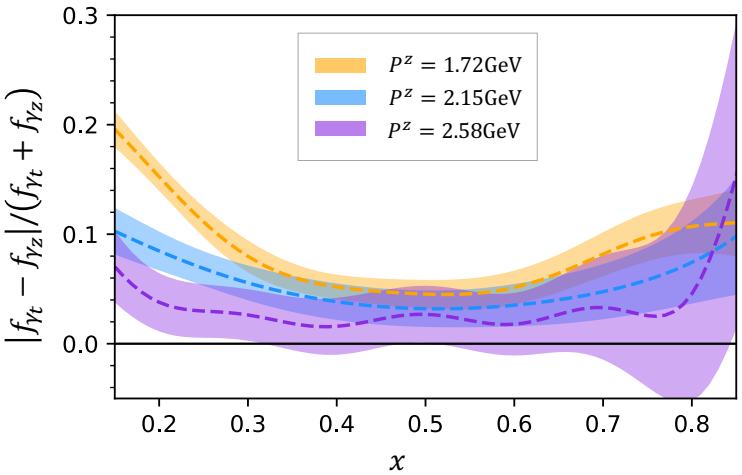

- Asymptotic behavior when P^z increases.
- The ratio shows the higher power corrections.
- There are large higher power corrections near the endpoint regions.

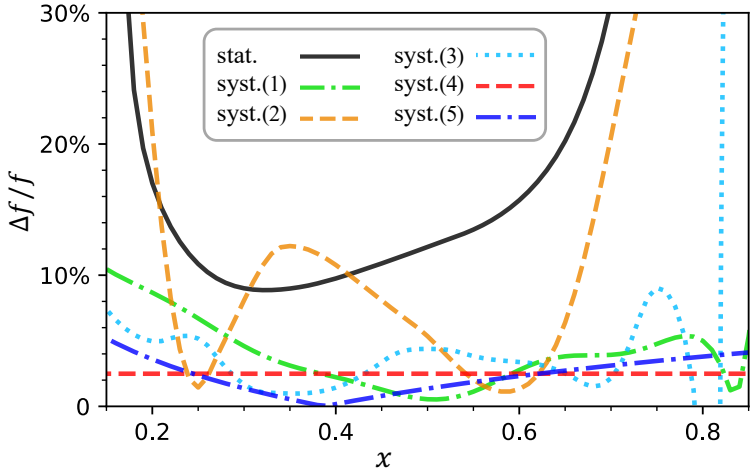

Source of systematical uncertainties:

- Power corrections;
- Physical extrapolation;
- Long distance extrapolation;
- Intrinsic soft function;
- Collins-Soper kernel.

Comparison with Pheno: x-dependence

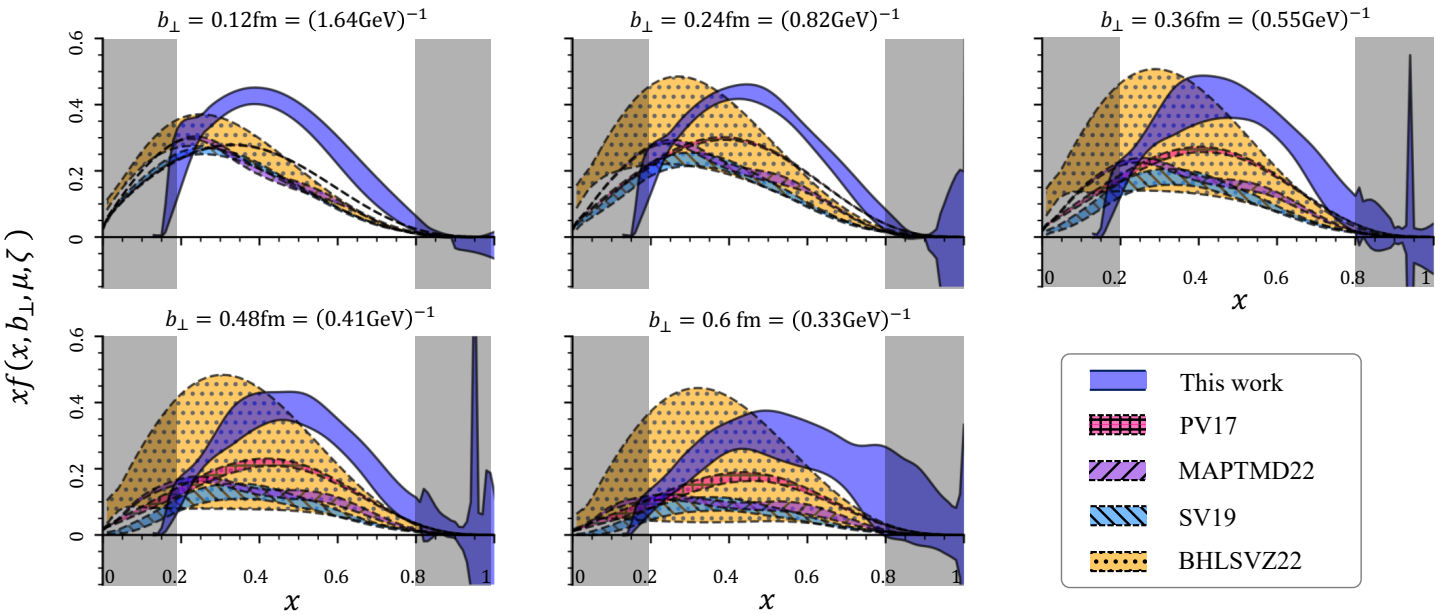

Bacchetta, et al. JHEP 06 (2017); Scimemi, et al. JHEP 06 (2020); Bury, et al. JHEP 10 (2022); Bacchetta, et al. JHEP 10 (2022)

- Preliminary lattice results consist with pheno results qualitatively.
- Shaded area cannot be predicted with LaMET.

Comparison with Pheno: Latest results

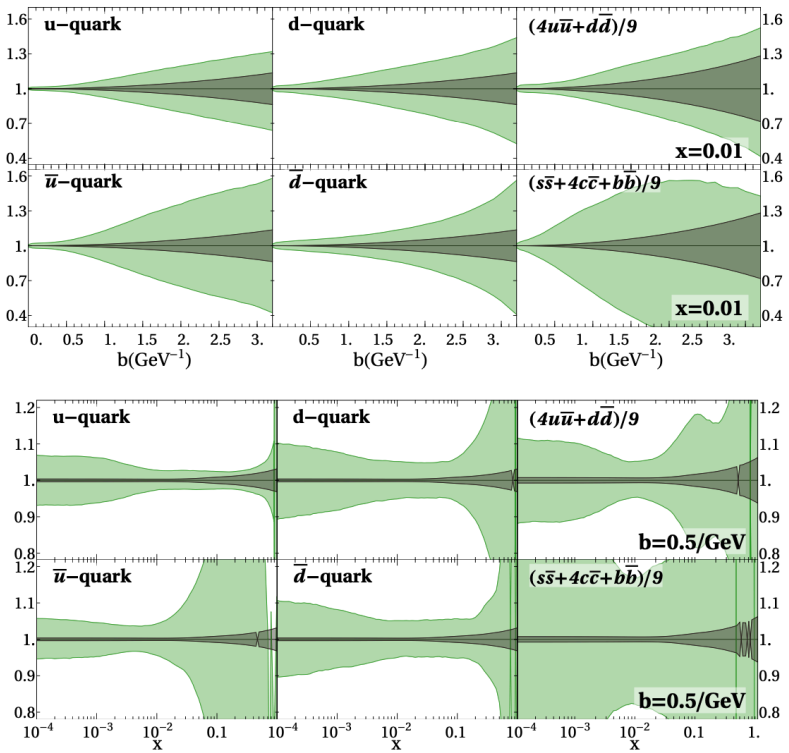

Figure 8. Sizes of the uncertainty bands in ART23 (green) in comparison to the those of the SV19 extraction (grey). The upper panel shows the b-dependence at $x = 0.01$. The lower panel shows the $x-$dependence at $b = 0.5$ GeV^{-1}.

V. Moos, I. Scimemi, A. Vladimirov and P. Zurita, 2305.07473

Comparison with Pheno: b-dependence

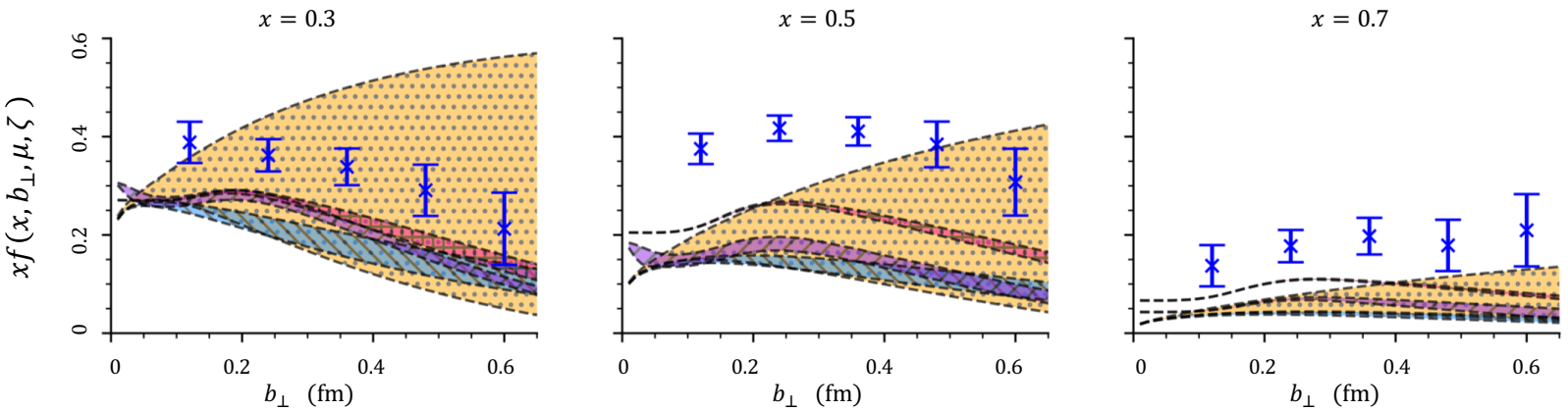

Bacchetta, et al. JHEP 06 (2017); Scimemi, et al. JHEP 06 (2020); Bury, et al. JHEP 10 (2022); Bacchetta, et al. JHEP 10 (2022)

- Both lattice and pheno results show a decreasing behavior in the b-dependence.
- Larger x corresponds to longer correlation length.

Discussion

Saturation: there are a lot of partons with small x fractions, they need to occupy more states with large transverse momentum.

Our results: large x — long correlation length

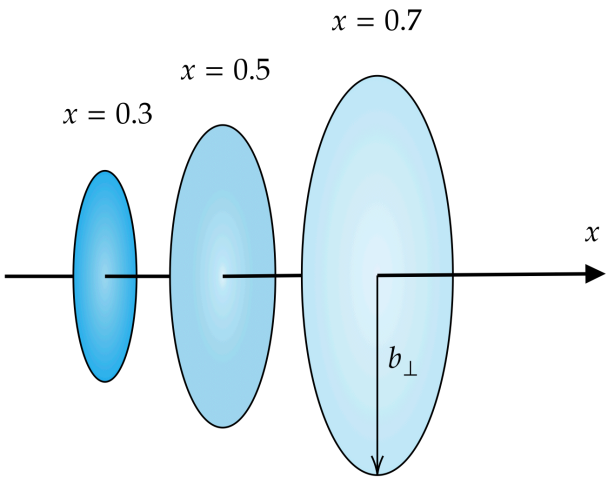

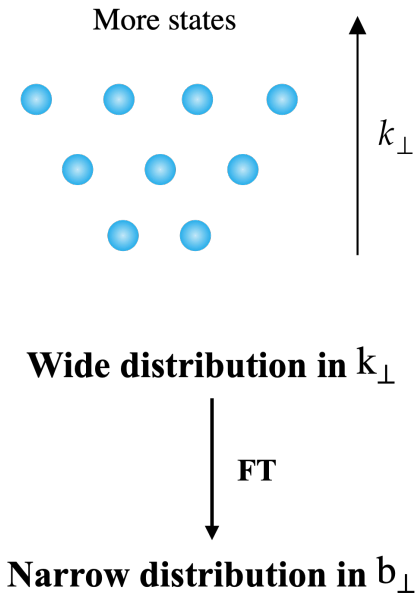

Improvements

Direction	Prospect
Discretization effects	Continuum limit, Lattice pert. theory
Transverse behavior	Small b problem, Confinement
Power correction	Larger γ factor
More	Higher loop calculation

X. Ji, Y. Liu and Y. Su, 2305.04416

Ó. del Río and A. Vladimirov, 2304.14440

Other TMDPDFs

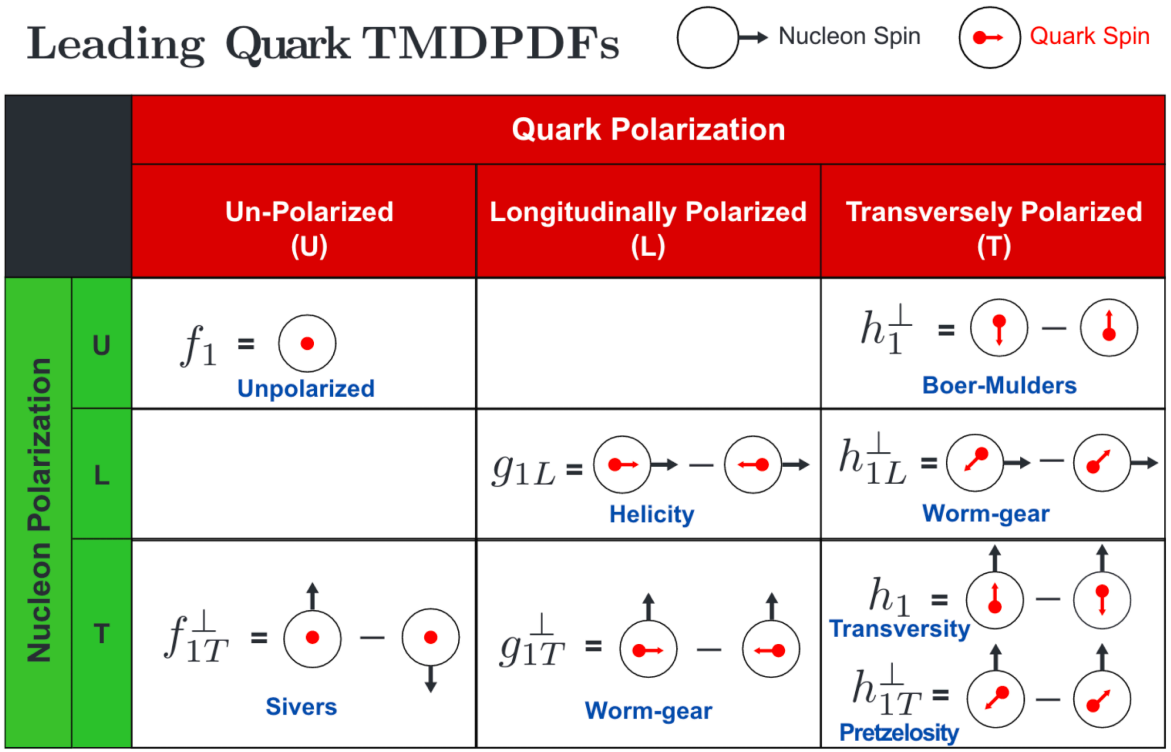

Thank You

Backup: Ground State Fit: Consistent results with different L

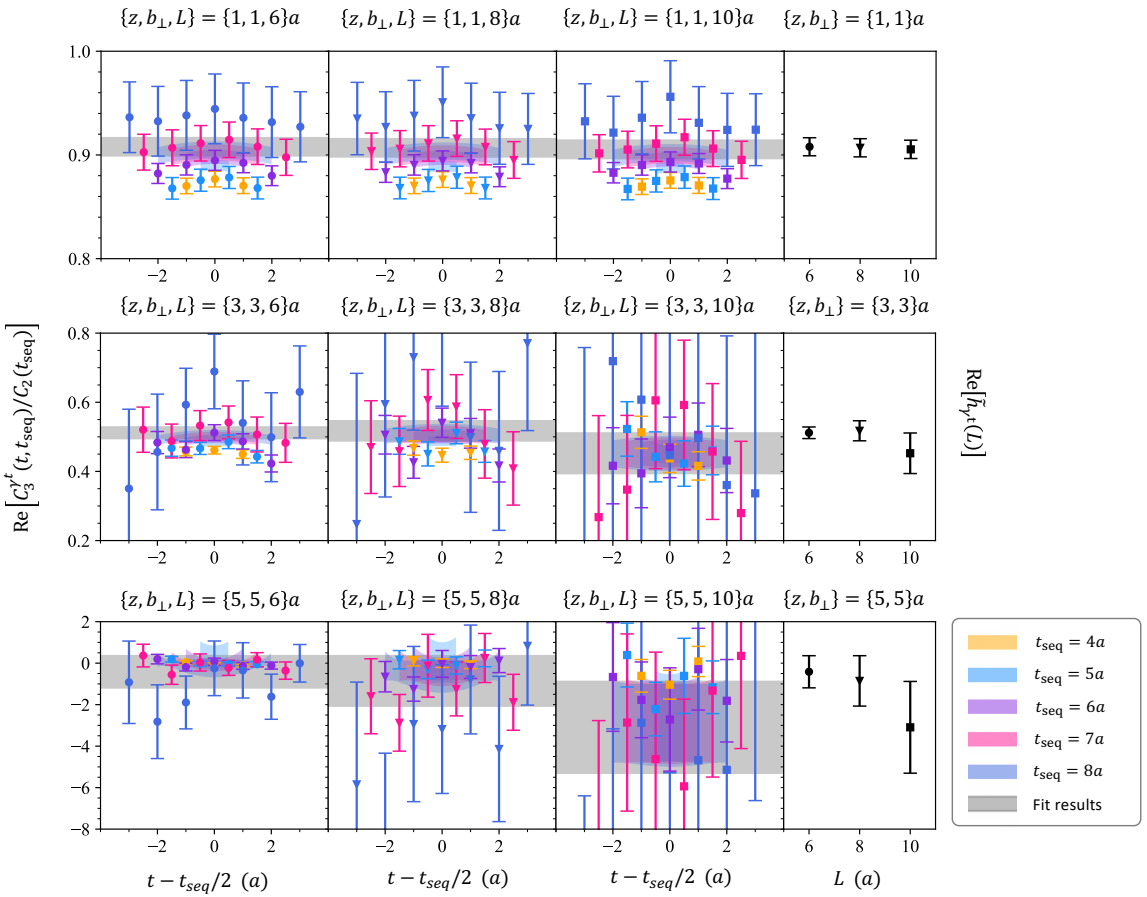

Backup: L-dependence

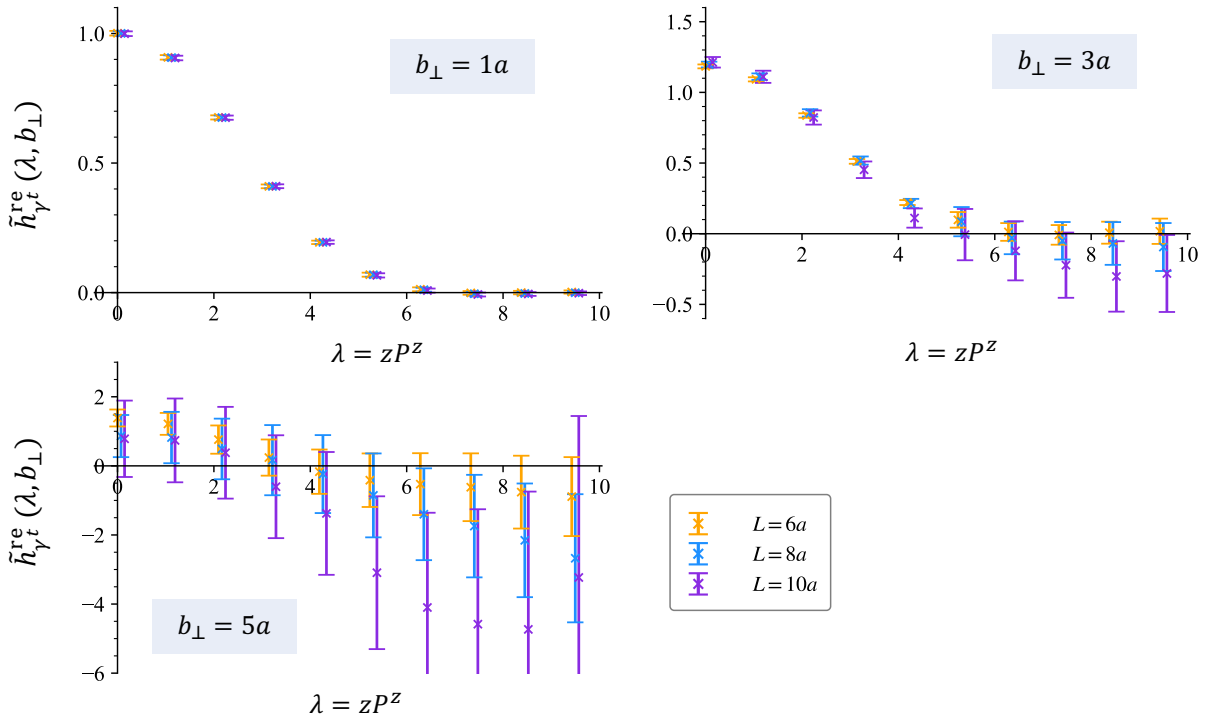

Backup: Extrapolation in the coordinate space

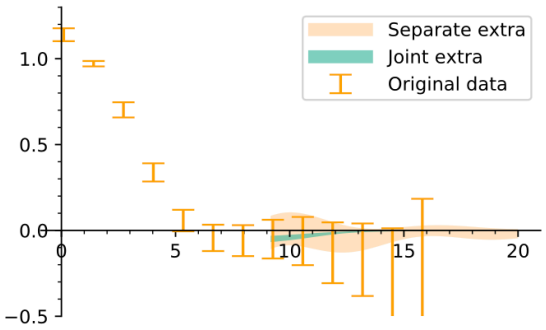

(a) $m_\pi = 220\text{MeV}$, $P^z = 2.15\text{GeV}$, $b_\perp = 5a$

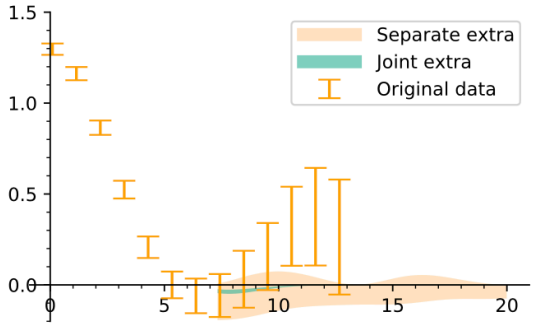

(b) $m_\pi = 220\text{MeV}$, $P^z = 1.72\text{GeV}$, $b_\perp = 5a$

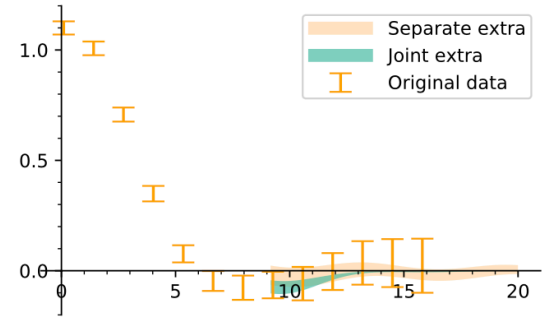

(c) $m_\pi = 220\text{MeV}$, $P^z = 2.15\text{GeV}$, $b_\perp = 3a$

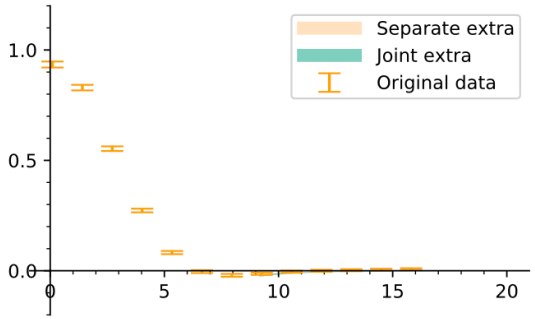

(d) $m_\pi = 220\text{MeV}$, $P^z = 2.15\text{GeV}$, $b_\perp = 1a$

Backup: Extrapolation Parameters

Fit results:

	m_1	m_2	n_1	n_2	λ_0	χ^2/d.o.f
$b = 1a$	$-8.8(3.7)$	$0.25(50)$	$0.909(39)$	$1.13(74)$	$2.63(38)$	1.0
$b = 2a$	$-6.3(2.9)$	$-3.9(5.5)$	$0.943(61)$	$2.37(68)$	$4.1(1.1)$	1.1
$b = 3a$	$-66(60)$	$-78(76)$	$0.89(12)$	$1.71(31)$	$2.42(85)$	1.4
$b = 4a$	$-8.0(4.4)$	$-3.3(2.9)$	$0.801(78)$	$1.55(38)$	$4.3(1.6)$	0.75
$b = 5a$	$-8.5(10)$	$-3.8(5.3)$	$0.84(16)$	$1.22(44)$	$4.4(2.8)$	0.57
Joint fit	–	–	$0.887(28)$	$1.65(12)$	$2.53(28)$	1.2

Backup: Ground state fit stability

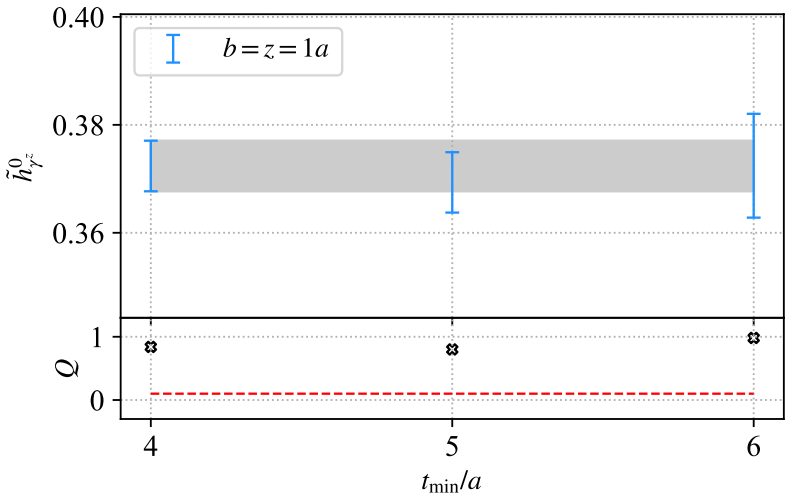

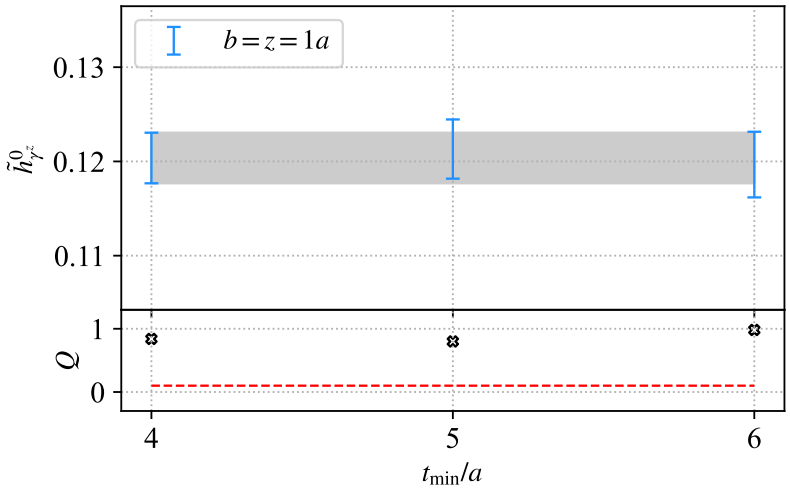

Backup: Lattice setup

a12m130: We use the valence tadpole improved clover fermion on the hypercubic (HYP) smeared 2 + 1 + 1 flavors MILC configurations with highly improved staggered quark (HISQ) sea and 1-loop Symanzik improved gauge action.

Backup: Dispersion Relation

$$E^2 = m^2 + c_1 \cdot P^2 + c_2 \cdot P^4$$

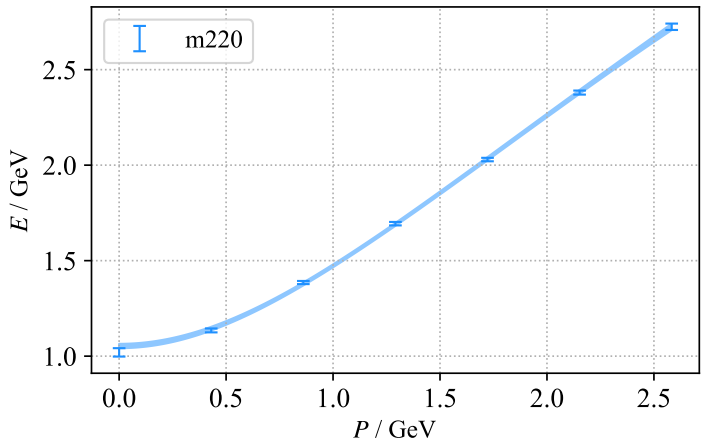

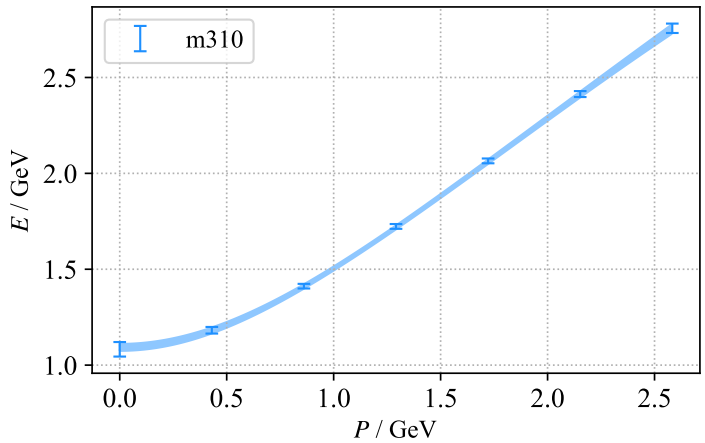

Figure 2: Dispersion relations.
m220:$Q = 0.19, c_1 = 1.081(20), c_2 = -0.0548(96)$;
m310:$Q = 1, c_1 = 1.087(28), c_2 = -0.053(13)$.